Parametric Analysis of Multi Source Feeding Flare Rolling and Corrugating Effects for H-Plane Horn Radiator

Ahmet S. Turk and Ozan Yurduseven

Department of Electronics and Communication Engineering
Yildiz Technical University, Istanbul, 34349, Turkey
Besiktas, 34349, Istanbul, Turkey
asturk@yildiz.edu.tr

Abstract ─ In this paper, radiation characteristics of H-plane sectoral horn antenna are treated systematically by investigation of the multi source feeding, flare wall rolling and corrugating effects. The analytical regularization method (ARM) is used to solve the problem of E-polarized wave diffraction in a fast and accurate way. The numerical procedure is initially verified by the analytical solutions, and the calculated field patterns are presented for the selected horn antenna configurations. Proper choices of the geometrical parameters, such as source position, back wall shape, multi source feed, metal thickness, and ridged and corrugated flares are proposed for the designers to reach high directivity, narrow beam, and suppressed side and back lobe levels.

Index Terms ─ Analytical regularization method, corrugated horn, flare rolling, horn antenna, multi source feeding.

I. INTRODUCTION

Horn structures are one of the most popular antenna technologies commonly used in wideband RF communication systems, high power microwave devices, electromagnetic compatibility tests, microwave and millimeter wave radars, and parabolic reflector feeder designs [1-6]. The radiation characteristics of horn antennas have been investigated starting from the analysis of principal configurations, and numerous practical types of the horn antennas have been developed in recent years [7-11]. The initial research methods were analytical techniques, which are primarily based on the mode-matching and aperture integration principals [3, 12]. However, the arbitrary shaped horn geometries used in practice were analyzed only by experiments or optical approximations [7]. Thus, direct numerical techniques such as, finite difference time domain (FDTD), finite element method (FEM), method of moments (MoM), and hybrid algorithms are considered more versatile and usable in practical models [13-15]. Nevertheless, they often require a long computing time especially for large size horn designs and wide band analysis [4,14]. Moreover, MoM and FEM can cause unstable numerical process for some structures due to reducing the boundary value problem (BVP) to the algebraic equation set of the first kind that usually has a singular kernel [16]. Hence, the analytical-numerical approaches that transform the ill-conditioned integral equation of first kind into a well-conditioned one of second kind are preferred to solve the matrix equation numerically by truncation method with fast convergence to obtain fast and reliable solutions [9,16]. On this scope, the analytical regularization method (ARM) is proposed for calculation of the horn radiation [17]. The primary analysis of the H-plane horn antenna has been demonstrated by Turk with investigation of the effects of essential parameters such as, different waveguide lengths, widths, flare angles and aperture sizes to characterize the radiation pattern [18].

This study deals with the parametric analysis of radiation from two-dimensional (2D) H-plane horn structure for different geometrical configurations of line source feeder positioning, back wall shaping, multi source locating, and flare rolling and corrugating. The principal aim is to characterize the radiation pattern to achieve low side and back lobe levels. For this purpose, the BVP is essentially formulated with respect to *z*-

component of the electric field satisfying Helmholtz's equation with Dirichlet boundary condition, and the ARM procedure is applied to obtain fast, accurate, and reliable results [5,18]. The numerical results are presented in figures, including performance comparisons with 3D numerical techniques.

II. ARM FORMULATION

The H-plane horn antenna is primarily considered as a perfectly conducting cylindrical obstacle, which is smooth, longitudinally homogeneous, and infinitely long in *z*-direction. The XOY cross section of the structure shown in Fig. 1 is denoted by the closed contour *S*. Let us assume the scalar wave does not vary along *z*-axis. In this case, the scalar diffraction problem of such an object corresponds to the 2D Dirichlet boundary condition for incidence of E-polarized wave. Hence, the incident and scattered scalar wave functions ($u^i(p)$ and $u^s(p)$) should satisfy the Helmholtz equation and the Dirichlet boundary condition given in Eq. (1) and Eq. (2) [16].

$$(\Delta + k^2)u^s(p) = 0, \quad p \in R^2 \setminus S, \tag{1}$$

$$u^{s(+)}(p) = u^{s(-)}(p) = -u^i(p), \quad p \in S, \tag{2}$$

where, *S* is the smooth contour of the structure domain in 2D space R^2 that belongs to the smoothness class $C^{2,\alpha}$ [16]. $u^{s(+)}(p)$ and $u^{s(-)}(p)$ are limiting values of $u^s(p)$ in the inner and the outer sides of *S*, respectively. The solution of the BVP is written in Eq. (3) using the Green's formula and the related boundary condition defined in Eq. (2).

$$-\frac{i}{4}\int_S \left[H_0^{(1)}(k\,|q-p|)Z(p)\right]dl_p = -u^i(q), \quad q, p \in S, \tag{3}$$

where,

$$Z(p) = \frac{\partial u^{s(-)}(p)}{\partial n} - \frac{\partial u^{s(+)}(p)}{\partial n}, \quad p \in S. \tag{4}$$

n is the unit outward with respect to *S* normal of the point *p*. The unknown function *Z(p)* is constructed by solving Eq. (3) and using parameterization of the *S* contour specified by the function $\eta(\theta)=(x(\theta),y(\theta))$ that smoothly parameterizes the contour *S* by the points of $\theta\in[-\pi,\pi]$. The functions $x(\theta)$, $y(\theta)$ are Cartesian-like coordinates of the point $\eta(\theta)\in S$, which are supposed to be infinitely smooth functions after their 2π-periodical continuation on $(-\infty,\infty)$. The parametric representation of the integral equation of the first kind in Eq. (3) can be equivalently rewritten as,

$$\frac{1}{2\pi}\int_{-\pi}^{\pi}\left\{\ln\left|2\sin\frac{\theta-\tau}{2}\right| + K(\theta,\tau)\right\}Z_D(\tau)d\tau = g(\theta), \quad \theta\in[-\pi,\pi], \tag{5}$$

by means of the following $\eta(\theta)$ transformations:

$$Z_D(\theta) = \left([x'(\theta)]^2 + [y'(\theta)]^2\right)^{1/2} Z(\eta(\theta)), \quad \theta\in[-\pi,\pi], \tag{6}$$

$$|q-p| = \left\{[x(\theta)-x(\tau)]^2 + [y(\theta)-y(\tau)]^2\right\}^{1/2}, \quad \theta\in[-\pi,\pi], \tag{7}$$

$$g(\theta) = -u^i(\eta(\theta)), \qquad \theta\in[-\pi,\pi]. \tag{8}$$

In Eq. (5), the unknown function is $Z_D(\tau)$, the given function is $g(\theta)$, and $K(\theta,\tau)$ function is the rather smooth section of the Green's function in comparison with the logarithmic part that contains the main singularity of this equation [17]. The functions are represented by their Fourier series expansions with $k_{s,m}$, z_m, g_m coefficients, as defined in set of Eqs. (9)-(12).

$$K(\theta,\tau) = \sum_{s=-\infty}^{\infty}\sum_{m=-\infty}^{\infty} k_{sm}e^{i(s\theta+m\tau)}, \quad \theta\in[-\pi,\pi], \tag{9}$$

$$\ln\left|2\sin\frac{\theta-\tau}{2}\right| = -\frac{1}{2}\sum_{\substack{n=-\infty\\ n\neq 0}}^{\infty}|n|^{-1}e^{in(\theta-\tau)}, \quad \theta\in[-\pi,\pi], \tag{10}$$

$$Z_D(\tau) = \sum_{n=-\infty}^{\infty} z_n e^{in\tau}, \quad \tau\in[-\pi,\pi], \tag{11}$$

$$g(\theta) = \sum_{n=-\infty}^{\infty} g_n e^{in\theta}, \quad \theta\in[-\pi,\pi]. \tag{12}$$

Finally, one can obtain an infinite system of the linear algebraic equations of the second kind given in Eq. (13).

$$\hat{z}_s + \sum_{m=-\infty}^{\infty}\hat{k}_{s,m}\hat{z}_m = \hat{g}_s, \quad s = \pm1, \pm2, .. \tag{13}$$

where,

$$\hat{k}_{s,m} = -2\tau_s\tau_m\left[k_{s,-m} + (1/2)\delta_{s,0}\delta_{m,0}\right],$$
$$\hat{z}_n = \tau_n^{-1}z_n, \qquad \hat{g}_s = -2\tau_s g_s. \tag{14}$$

Here, $\delta_{s,n}$ is the Kronecker delta function. As a result, Eq. (13) leads to the generic form of equation of the second kind that guarantees the convergence and stability of this numerical process. Therefore, the scattered field $u^s(q)$ for $q\in R^2$ are calculated by the integral equation representation of the Eq. (3) with any required

accuracy by the truncation method [17].

III. PARAMETRIC DESIGN OF H-PLANE HORN ANTENNA

The described ARM procedure is derived for the selected horn antenna types, and the geometrical cross-section of the horn is modeled by ARM as a closed contour L that goes from point A to point T and back to A corresponding to $\theta \in [-\pi, \pi]$, as illustrated in Fig. 1. The relation between l and θ is formulated in Eq. (15).

$$\left.\begin{aligned} & l = (\theta + \pi) L / 2\pi \\ & l \in [0, L] \to (\theta, \tau) \in [-\pi, \pi] \end{aligned}\right\}. \tag{15}$$

Then, the effects on radiation characteristics of the treated design parameters such as, multi source positioning, feeder back wall shaping, and flare wall rolling and corrugating are determined.

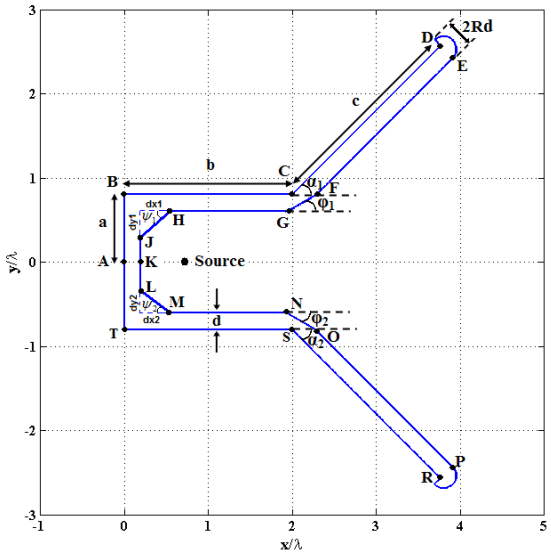

Fig. 1. XOY-plane geometry of H-plane horn.

The horn structure consists of totally 18 contour parts, which are defined in Table 1 and 2. The parameterization of the contour line is implemented separately from point A to T, and back to A by means of the variable $l \in [0, L]$ as follows:

$$x = 0, \;\; y = l - L_{AB} + a, \;\; l \in [AB) \tag{16}$$

$$x = l - L_{AB}, \quad y = a \quad , l \in [BC) \tag{17}$$

$$\left.\begin{aligned} x &= (l - L_{BC}) \cos\alpha_1 + b \\ y &= (l - L_{BC}) \sin\alpha_1 + a \end{aligned}\right\}, l \in [CD) \tag{18}$$

$$\left.\begin{aligned} x &= \left[\frac{d}{2}\sin\alpha_1 + b + c\cos\alpha_1\right] + R\frac{d}{2}\cos\left[\left(\frac{\pi}{2} + \alpha_1\right) - 2\left(\frac{l - L_{CD}}{Rd}\right)\right] + X_0 \\ y &= \left[-\frac{d}{2}\cos\alpha_1 + a + c\sin\alpha_1\right] + R\frac{d}{2}\sin\left[\left(\frac{\pi}{2} + \alpha_1\right) - 2\left(\frac{l - L_{CD}}{Rd}\right)\right] + Y_0 \\ X_0 &= -(R-1)\frac{d}{2}\sin\alpha_1, \quad Y_0 = (R-1)\frac{d}{2}\cos\alpha_1 \end{aligned}\right\}, l \in [DE) \tag{19}$$

$$\left.\begin{aligned} x &= b + d\sin\alpha_1 + [c - l + L_{DE}]\cos\alpha_1 \\ y &= a - d\cos\alpha_1 + [c - l + L_{DE}]\sin\alpha_1 \end{aligned}\right\}, \; l \in [EF) \tag{20}$$

$$\left.\begin{aligned} x &= d/\sin\alpha_1 + b - (l - L_{EF})\cos\varphi_1 \\ y &= a - (l - L_{EF})\sin\varphi_1 \end{aligned}\right\}, l \in [FG) \tag{21}$$

$$x = -l + L_{FG} + b - db_1, \quad y = a - d \quad , l \in [GH) \tag{22}$$

$$\left.\begin{aligned} x &= (-l + L_{GH})\cos(\psi_1) + d + dx_1, \\ y &= a - d - (l - L_{GH})\sin(\psi_1), \end{aligned}\right\}, l \in [HJ) \tag{23}$$

$$x = d, \quad y = -l + L_{HJ} + a - d - dy_1, l \in [JK) \tag{24}$$

$$x = d, \quad y = -l + L_{JK}, \; l \in [KL) \tag{25}$$

$$\left.\begin{aligned} x &= d + (l - L_{KL})\cos(\psi_2) \\ y &= -a + d + dy_2 - (l - L_{KL})\sin(\psi_2) \end{aligned}\right\}, l \in [LM) \tag{26}$$

$$x = l - L_{LM} + d + dx_1, \quad y = -a + d \;, \; l \in [MN) \tag{27}$$

$$\left.\begin{aligned} x &= b - db_2 + (l - L_{MN})\cos\varphi_2 \\ y &= -a + d - (l - L_{MN})\sin\varphi_2 \end{aligned}\right\}, \; l \in [NO) \tag{28}$$

$$\left.\begin{aligned} x &= d/\tan\alpha_2 + b + (l - L_{NO})\cos\alpha_2 + 0.5d\sin\alpha_2 \\ y &= -a - (l - L_{NO})\sin\alpha_2 \end{aligned}\right\}, l \in [OP) \tag{29}$$

$$\left.\begin{aligned} x &= \frac{d}{2}\sin\alpha_2 + b + c\cos\alpha_2 + R\frac{d}{2}\cos\left[\frac{\pi}{2} - \alpha_2 - 2\left(\frac{l - L_{OP}}{Rd}\right)\right] + X_0 \\ y &= -\left(-\frac{d}{2}\cos\alpha_2 + a + c\sin\alpha_2\right) + R\frac{d}{2}\sin\left[\frac{\pi}{2} - \alpha_2 - 2\left(\frac{l - L_{OP}}{Rd}\right)\right] + Y_0 \\ X_0 &= -(R-1)\frac{d}{2}\sin\alpha_2, \quad Y_0 = -(R-1)\frac{d}{2}\cos\alpha_2 \end{aligned}\right\}, l \in [PR) \tag{30}$$

$$\left.\begin{aligned} x &= -(l - L_{PR})\cos\alpha_2 + b + c\cos\alpha_2 \\ y &= (l - L_{PR} - c)\sin\alpha_2 - a \end{aligned}\right\}, l \in [RS) \tag{31}$$

$$x = -l + L_{RS} + b \quad y = -a \quad , \; l \in [ST) \tag{32}$$

$$x = 0, \quad y = l - L_{ST} - a \quad , \; l \in [TA) \tag{33}$$

The horn antenna is supposed to be excited by line source(s) located in the waveguide region at specified pin inset apart from the back wall. Thus, the incident wave at any (*x,y*) coordinate of the horn structure ($u^i(x,y)$) is calculated by the line source radiation formula.

Table 1: Parametric definitions of horn contour

No	Region	Definition
1	*AB*	$-\pi \le \theta < -\pi + 2L_{AB}\,\pi/L$
2	*BC*	$-\pi + 2L_{AB}\,\pi/L \le \theta < -\pi + 2L_{BC}\,\pi/L$
3	*CD*	$-\pi + 2L_{BC}\,\pi/L \le \theta < -\pi + 2L_{CD}\,\pi/L$
4	*DE*	$-\pi + 2L_{CD}\,\pi/L \le \theta < -\pi + 2L_{DE}\,\pi/L$
5	*EF*	$-\pi + 2L_{DE}\,\pi/L \le \theta < -\pi + 2L_{EF}\,\pi/L$
6	*FG*	$-\pi + 2L_{EF}\,\pi/L \le \theta < -\pi + 2L_{FG}\,\pi/L$
7	*GH*	$-\pi + 2L_{FG}\,\pi/L \le \theta < -\pi + 2L_{GH}\,\pi/L$
8	*HJ*	$-\pi + 2L_{GH}\,\pi/L \le \theta < -\pi + 2L_{HJ}\,\pi/L$
9	*JK*	$-\pi + 2L_{HJ}\,\pi/L \le \theta < -\pi + 2L_{JK}\,\pi/L$
10	*KL*	$-\pi + 2L_{JK}\,\pi/L \le \theta < -\pi + 2L_{KL}\,\pi/L$
11	*LM*	$-\pi + 2L_{KL}\,\pi/L \le \theta < -\pi + 2L_{LM}\,\pi/L$
12	*MN*	$-\pi + 2L_{LM}\,\pi/L \le \theta < -\pi + 2L_{MN}\,\pi/L$
13	*NO*	$-\pi + 2L_{MN}\,\pi/L \le \theta < -\pi + 2L_{NO}\,\pi/L$
14	*OP*	$-\pi + 2L_{NO}\,\pi/L \le \theta < -\pi + 2L_{OP}\,\pi/L$
15	*PR*	$-\pi + 2L_{OP}\,\pi/L \le \theta < -\pi + 2L_{PR}\,\pi/L$
16	*RS*	$-\pi + 2L_{PR}\,\pi/L \le \theta < -\pi + 2L_{RS}\,\pi/L$
17	*ST*	$-\pi + 2L_{RS}\,\pi/L \le \theta < -\pi + 2L_{ST}\,\pi/L$
18	*TA*	$-\pi + 2L_{ST}\,\pi/L \le \theta < \pi$

IV. NUMERICAL RESULTS

The parametric analysis of the horn antenna is focused on the investigation of the effects of feeder positioning, back wall shaping, multi source locating, and rolling and corrugating of the flare wall to characterize the radiation pattern. First aim of this work is to minimize the side and back lobes. Before we demonstrate the numerical results, it is important to explain the reliability of the generic ARM algorithm, which has already been verified with analytical results by achieving very good agreements for the cases of plane wave scattering from a circular cylinder and radiation from open ended waveguide [5,18]. The ARM results of one horn type were also compared with analytical solutions additionally, and good agreements were obtained as shown in Fig. 2.

Table 2: Segment lengths of the contour regions

No	Region	Segment Length
1	*AB*	$L_{AB} = a$
2	*BC*	$L_{BC} = L_{AB} + b$
3	*CD*	$L_{CD} = L_{BC} + c$
4	*DE*	$L_{DE} = L_{CD} + \pi Rd/2$
5	*EF*	$L_{EF} = L_{DE} + c - d/\tan\alpha_1$
6	*FG*	$L_{FG} = L_{EF} + d/\sin\varphi_1$
7	*GH*	$L_{GH} = L_{FG} + b - db_1 - d - dx$
8	*HJ*	$L_{HJ} = L_{GH} + \sqrt{(dx_1^2 + dy_1^2)}$
9	*JK*	$L_{JK} = L_{HJ} + a - d - dy_1$
10	*KL*	$L_{KL} = L_{JK} + a - d - dy_2$
11	*LM*	$L_{LM} = L_{KL} + \sqrt{(dx_2^2 + dy_2^2)}$
12	*MN*	$L_{MN} = L_{LM} + b - db_2 - dx_2 - d$
13	*NO*	$L_{NO} = L_{MN} + d/\sin\varphi_2$
14	*OP*	$L_{OP} = L_{NO} + c - d/\tan\alpha_2$
15	*PR*	$L_{PR} = L_{OP} + \pi Rd/2$
16	*RS*	$L_{RS} = L_{PR} + c$
17	*ST*	$L_{ST} = L_{RS} + b$
18	*TA*	$L = L_{ST} + a$
$db_{1,2} = d/\tan\varphi_{1,2} - d\tan\alpha_{1,2}$		

The analysis results for different back wall corner angle, ridged flare, wall thickness, corrugated teeth length, line source positioning at horizontal and vertical axis, and multi source feeding configurations are presented in Fig. 3, Fig. 4, Fig. 5, Fig. 6, Fig. 7, Fig. 8, and Fig. 9, respectively. The major effects are briefly commented as that; the back wall corner can suppress the first side lobes up to 5 dB (see Fig. 3), the flare rolling can decrease both side and back lobes between 5-10 dB (see Fig.4), the thick metal walls can yield 15 dB suppressed back lobes (see Fig. 5), and the corrugating teeth can reach narrowed main beam width with about 5-10 dB improved side and back lobe levels (see Fig. 6). Figsures 7-9 indicate the back lobe suppression and side lobe asymmetry performances of pin inset and multi-pin localizations along *x* and *y* axis.

Figure 10 proposes a flare ridged horn design combined with triple source feeding to obtain 20 dB more suppressed side lobe levels. The multi source fed corrugated horn design shown in Fig. 11 is another antenna proposal that can successfully achieve -40 dB back lobe and -15 dB side lobe levels.

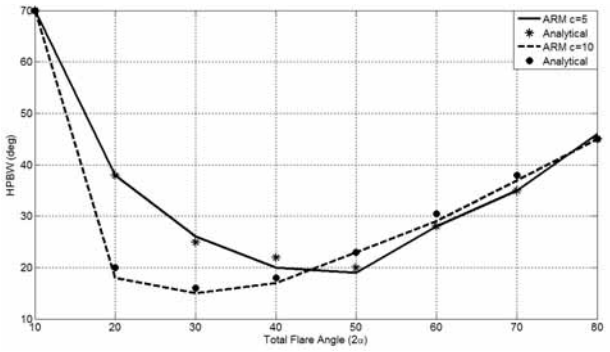

Fig. 2. Half-power beam width plots of ARM calculations and analytical results [3].
(Type 1: a= 0.6λ, b= 4λ, d= 0.1λ, R= 1, α_1= α_2= φ_1= φ_2= α, Ψ_1 = Ψ_2 = 0º)

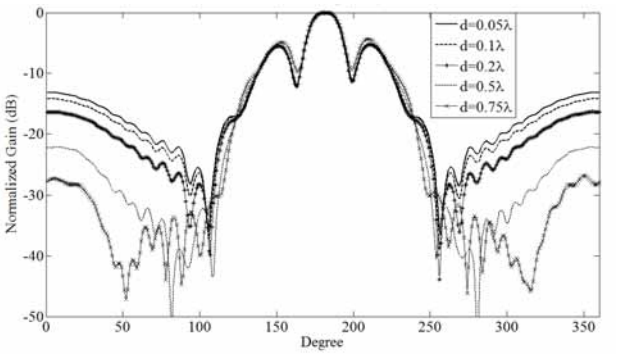

Fig. 5. Normalized radiation patterns of the horn for different wall thicknesses.
(Type 2: a= 1.1λ, b= 2λ, c= 4λ, R= 1, α_1= α_2= 45º, φ_1= φ_2= 45º, Ψ_1 = Ψ_2 = 0º)

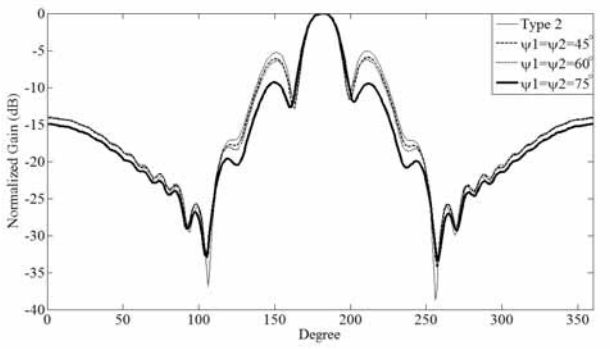

Fig. 3. Normalized radiation patterns of the horn for different back wall corner angles.
(Type 2: a= 1.1λ, b= 2λ, c= 4λ, d= 0.1λ, R= 1, α_1= α_2= 45º, φ_1= φ_2= 45º, dx= 0.25λ)

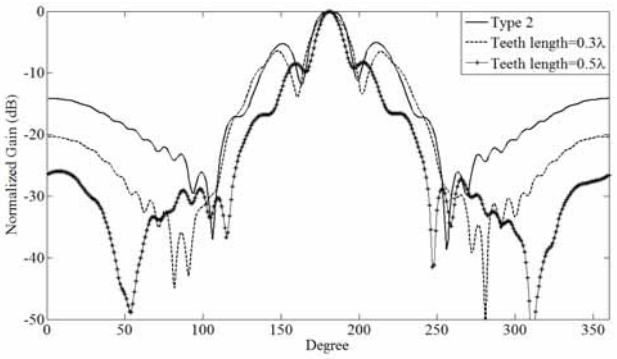

Fig. 6. Normalized radiation patterns of the corrugated horn for different lengths of the teeth.
(Type 2: a= 1.1λ, b= 2λ, c= 4λ, d= 0.1λ, R= 1, α_1= α_2= 45º, Ψ_1 = Ψ_2 = 0º)

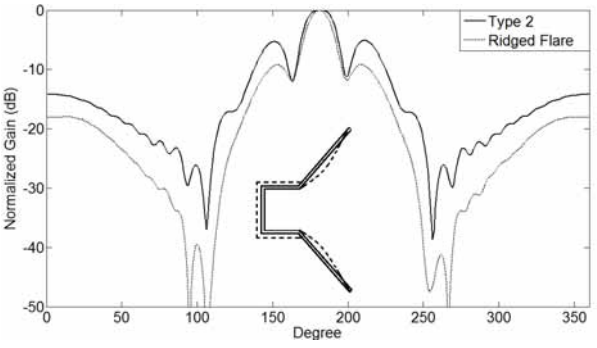

Fig. 4. Normalized radiation pattern of flare rolled type horn.
(Type 2: a= 1.1λ, b= 2λ, c= 4λ, d= 0.1λ, R= 1, α_1= α_2= 45º, φ_1= φ_2= 45º, Ψ_1 = Ψ_2 = 0º)

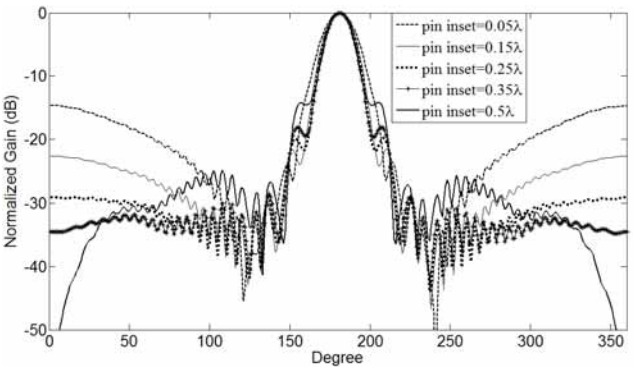

Fig. 7. Normalized radiation patterns of the horn for different pin insets (along x-axis).
(Type 3: a= 0.481λ, b= 2.6λ, c= 8.664λ, d= 0.1λ, α_1= α_2= 11.18º, φ_1= φ_2= 11.18º, Ψ_1 = Ψ_2 = 0º)

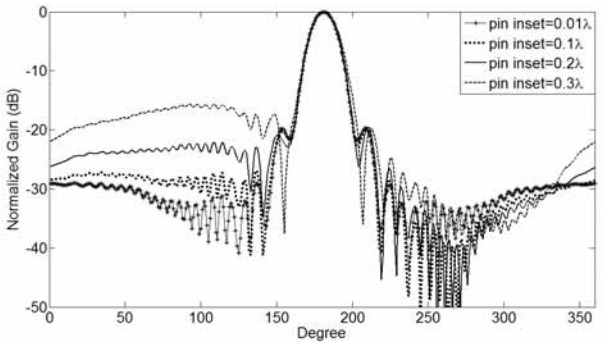

Fig. 8. Normalized radiation patterns of the horn for different pin insets (along *y*-axis).
(Type 3: a= 0.481λ, b= 2.6λ, c= 8.664λ, d= 0.1λ, $\alpha_1 = \alpha_2 = 11.18º$, $\varphi_1 = \varphi_2 = 11.18º$, $\Psi_1 = \Psi_2 = 0º$)

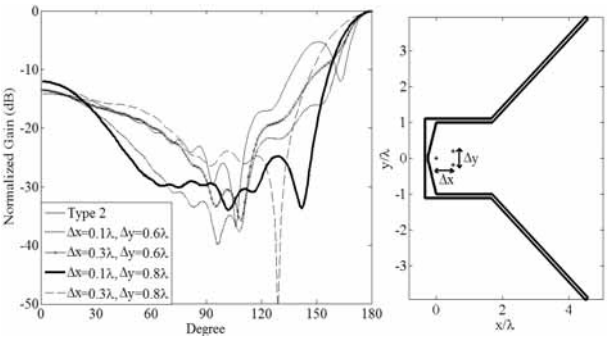

Fig. 9. Normalized radiation patterns of the horn for different triple line source feeding configurations.
(Type 2: a= 1.1λ, b= 2λ, c= 4λ, d= 0.1λ, R= 1, $\alpha_1 = \alpha_2 = 45º$, $\varphi_1 = \varphi_2 = 45º$, $\Psi_1 = \Psi_2 = 75º$)

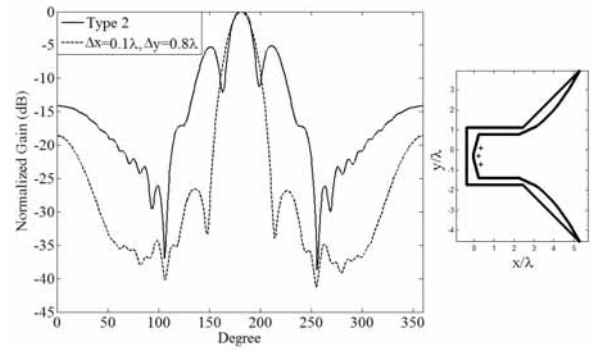

Fig. 10. Normalized radiation pattern of the flare ridged horn version with triple line source feeding.

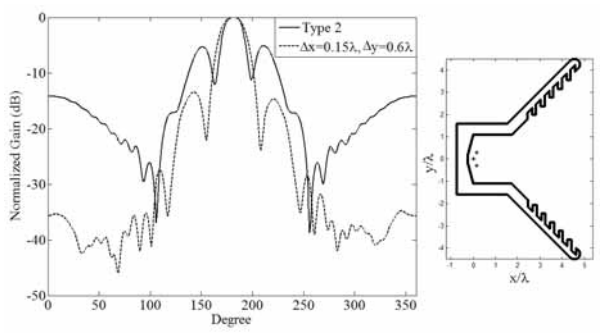

Fig. 11. Normalized radiation pattern of the corrugated horn version with triple line source feeding.

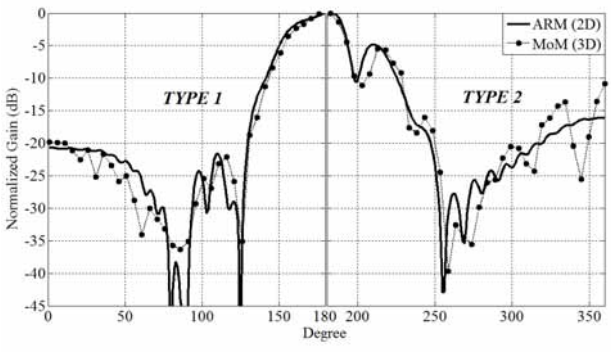

Fig. 12. Comparisons of radiation patterns calculated by 2D ARM and 3D MoM simulator.
(a) Type 1: a= 0.6λ, b= 4λ, c= 4λ, d= 0.1λ, R= 1, $\alpha_1 = \alpha_2 = 45º$
(b) Type 2: a= 1.1λ, b= 2λ, c= 4λ, d= 0.1λ, R= 1, $\alpha_1 = \alpha_2 = 45º$

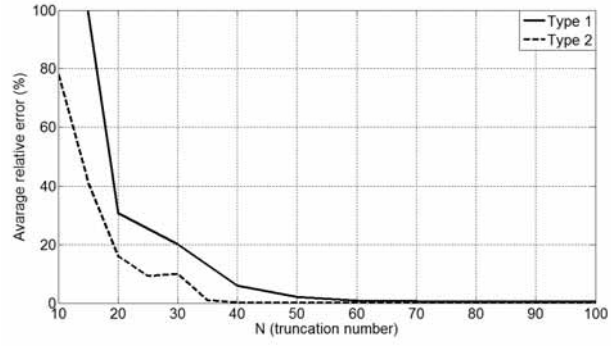

Fig. 13. Average of relative errors in numerical calculations (demonstrated for two horn types).

Finally, the 2D ARM solutions of two different horn types are compared with 3D MoM simulator results. The coherency observed in Fig. 12 implies that ARM is a useful technique due to

fast convergence and short calculation times (see Table 3 and Fig. 13), especially for rough model design and wide band analysis of the horn antennas.

Table 3: Computation times of ARM and 3D MoM simulator (2.53 GHz, 4 GB RAM)

Type	Truncation Number (*N*)	Computation Time	
		2D ARM	3D MoM
1	40	16.92 sec.	13 min. 48 sec.
	60	51.18 sec.	
2	40	16.92 sec.	12 min. 45 sec.
	60	51.18 sec.	
3	40	16.92 sec.	16 min. 23 sec.
	60	51.18 sec.	

V. CONCLUSION

This paper has presented the parametric analysis of the radiation characteristics of the H-plane horn antenna essentially for the geometric versions of multi source feeding, flare rolling, and corrugating. The analytical regularization method is used to perform 2-D analysis of the E-polarized electromagnetic wave scattering problem. The analysis results of different back wall corner angle, ridged flare, wall thickness, corrugated tooth length, vertical and horizontal line source positioning, multi source feeding configurations, and combined proposals are demonstrated on the radiation patterns. The main goal of this work is to provide systematic information for the horn designers to attain desired antenna patterns, such as high gain, narrow beam, and suppressed side and back lobes, in a fast and accurate way.

ACKNOWLEDGMENT

The authors would like to thank to Dr. Yury A. Tuchkin for the contribution in this study.

REFERENCES

[1] M. I. Skolnik, "*Radar handbook,*" 2nd ed., McGraw-Hill, 1990.

[2] T. A. Milligan, "Modern Antenna Design," 2nd ed., *IEEE Press*, John Wiley & Sons, 2005.

[3] C. A. Balanis, "*Antenna Theory Analysis and Design,*" 3rd ed., John Wiley & Sons, 2005.

[4] W. Ewe, L. Li, Q. Wu, and M. Leong, "Analysis of Reflector and Horn Antennas Using Adaptive Integral Methods," *IEICE Trans.* Comm., vol. E88-B, no.6, 2005.

[5] A. S. Turk, "Analysis of aperture illumination and edge rolling effects for parabolic reflector antenna design," *Int. J. Electronics Communications (AEÜ)*, vol. 60, pp. 257-266, 2006.

[6] C. Chang, X. X. Zhu, and Z. Q. Zhang, "Design and experiments of the GW high-power microwave feed horn," *Progress In Electromagnet. Research (PIER)*, vol. 101, pp. 157-171, 2010.

[7] M. Hamid and A. Al-Sulaiman, "New types of dielectric-loaded horn antennas," *Int. Journal of Electronics*, vol. 55, pp. 729-750. 1983.

[8] E. A. Parker, B. Philips, and R. J. Langley, "Experimental variable beam width horn," *Electronic Letters*, vol. 31, pp. 1539-1540, 1995.

[9] V. P. Chumachenko and A. S. Turk, "Radiation characteristics of wide-angle H-plane sectoral horn loaded with dielectric of multiangular shape," *Int. Journal Electronics*, vol. 88, no. 1, pp. 91-101, 2001.

[10] V. Jamnejad and A. Hoorfar, "Design of corrugated horn antennas by evolutionary optimization techniques," *IEEE Antennas and Wireless Prop. Letters*, vol. 3, pp. 276-279, 2004.

[11] D. R. Heydari, H. R. Hassani, and A. R. Mallahzadeh, "A new 2-18 GHz quad-ridged horn antenna," *Progress In Electromagnetics Research (PIER)*, vol. 81, pp. 183-195, 2008.

[12] S. Maci, P. Ya. Ufimtsev, and R. Tiberio, "Equivalence between physical optics and aperture integration for radiation from open-ended waveguides," *IEEE Trans. Antennas Propagation*, vol. 45, no. 1, pp. 183-185, 1997.

[13] C. Reig, E. A. Navarro, and V. Such, "FDTD Analysis of E-sectoral horn antennas for broad-band applications," *IEEE Trans. Antennas Propagation*, vol. 45, pp. 1484-1487, 1997.

[14] F. Arndt, J. Brandt, V. Catina, J. Ritter, I. Rullhusen, J. Dauelsberg, U. Hilgefort, and

W. Wessel, "Fast CAD and optimization of waveguide components and aperture antennas by hybrid MM/FE/MoM/FD methods: State of the art and recent advances," *IEEE Trans. Microwave Theory Tech.*, vol. 52, no.1, 2004.

[15] D. Baumann, C. Fumeaux, P. Leuchtmann, and R. Vahldieck, "Finite-volume time-domain (FVTD) modelling of a broadband double-ridged horn antenna," *Int. J. Numerical Modelling*, vol. 17, pp. 285-298, 2004.

[16] Yu. A. Tuchkin, "Wave scattering by an open cylindrical screen of arbitrary profile with Dirichlet boundary value condition," *Soviet Physics Doclady*, vol. 30, pp. 1027-1030, 1985.

[17] E. Karacuha and A. S. Turk, "E-polarized scalar wave diffraction by perfectly conductive arbitrary shaped cylindrical obstacles with finite thickness," *Int. J. Infrared and Millimeter Waves*, vol. 22, pp. 1531-1546, 2001.

[18] A. S. Turk, O. M. Yucedag, and O. Yurduseven, "Parametric analysis of H-plane horn antenna radiation," Proc. 7th Int. Kharkiv Symposium on Physics and Engineering of Microwaves, Millimeter Submilimeter Waves (MSMW), *IEEE press*, Ukraine, 21-26 June 2010.

Ahmet Serdar Turk received the B.S. degree in Electronics-Communication Engineering from Yıldız Technical University, Istanbul, Turkey in 1996. He received M.S. and Ph.D. degrees in Electronics Engineering from Gebze Institute of Technology, Kocaeli-Turkey in 1998 and 2001, respectively. He joined the Scientific and Technical Research Council of Turkey (TUBITAK) in 1998.

He has been working on land mine detection systems as an impulse radar RF system and antenna designer since 1998. His research interests include horn, reflector, array, and ultra-wide band antenna designs in RF and microwave bands, numerical methods in electromagnetic wave scattering, high frequency surface wave radar, ground penetrating radar, and microwave and millimeter wave radar systems.

He is currently working as associated professor at Yıldız Technical University.

Ozan Yurduseven received the B.S. degree in Electronics- Communication Engineering from Yıldız Technical University, Istanbul, Turkey in 2009. His research interests include microwave antenna design and numerical techniques in electromagnetics, especially method of moments, analytical regularization method, and optimization of radar cross section.